

Functionally constrained tractography: Improved diffusion MRI-based fiber tractography using functional information

Xi Wu^{1,2}, Xu Ran², Adam Anderson², and Zhaohua Ding²

¹ Huaxi MRI Research center, Sichuan University, Chengdu, Sichuan, China, ² Vanderbilt University Institute of Imaging Science, Vanderbilt University, Nashville, Tennessee, United States

TARGET AUDIENCE

This work is intended for researchers interested in developing fiber tractography methods on the basis of diffusion MRI.

PURPOSE

Streamline fiber tractography suffers from many inherent limitations, one of which is the estimation uncertainty of the tracking direction and inaccurate tracking results from it¹. We proposed a modular addition to DTI tracking algorithm, which introduced resting state fMRI signals² to constrained the tracking direction estimation and reconstructed neuronal pathway more accurately and robustly.

METHODS

Image acquisition: Anatomical MRI: T1-weighted (T1w) images were obtained using a multi-shot gradient echo (GE) sequence with TR=8.9 ms, TE=4.6 ms, matrix size=256×256×170, and voxel size=1×1×1 mm³. DW-MRI: A single-shot, spin echo (SE), echo planar imaging (EPI) sequence was used to acquire DW-MRI data with $b=1000$ s/mm², 32 diffusion-sensitizing directions, TR=10 s, TE=60 ms, SENSE factor=3, matrix size=128×128×60, and voxel size=2×2×2 mm³. To improve the image signal-to-noise ratio, three repeated scans were acquired. fMRI: Images sensitive to BOLD contrast were acquired using a T₂^{*}-weighted GE EPI sequence and the following parameters: TR=2 s, TE=35 ms, matrix size=64×64, FOV=240×240 mm², 30 slices of 4.5 mm thickness with a 0.5 mm gap, and 200 dynamics.

Image preprocessing: First, the three repeated DW-MRIs were co-registered and averaged, from which diffusion tensor elements were calculated using linear least squares fitting³. Second, the resting state fMRI data were corrected for slice timing and head motion using standard spm2 tools (<http://www.fil.ion.ucl.ac.uk/spm/software/spm2>). Subject data with movement more than 2 mm of translation or 2° of rotation in any direction were excluded. The corrected data were then co-registered with the $b=0$ DW-MRI volume. For each subject, a global time course was removed by intensity normalization, i.e., equalizing the mean values of all volumes in the data. The voxels in the brain were low pass filtered with a cutoff frequency of 0.1 Hz. Spatio-temporal correlation tensors were constructed voxel-wise, as described in the subsection below, using Pearson's linear correlation coefficients (r) of BOLD signals and $C=r^2$.

Construction of spatial-temporal correlation tensors: The BOLD-sensitive MRI signal from within each voxel provides a time series that exhibits small amplitude fluctuations. The temporal correlation between pairs of voxels indicates their degree of synchronous variation. Assuming only a first tier neighborhood of 26 voxels is used, a direction vector connecting a voxel of interest and each voxel in the neighborhood is defined, which is subsequently normalized into a unit vector. For a spatio-temporal correlation tensor \mathbf{T} to be constructed, the estimated correlation C projected along a vector $\mathbf{n}_i(x_i, y_i, z_i)$ is $C_i=\mathbf{n}_i \cdot \mathbf{T} \cdot \mathbf{n}_i'$.

Let \mathbf{C} denote observed temporal correlations along the 26 directions, the relation between \mathbf{C} and \mathbf{T}_c can be expressed as $\mathbf{C}=\mathbf{M} \cdot \mathbf{T}_c$, where \mathbf{M} is a design matrix of size 26×6. The i^{th} row of \mathbf{M} has the form of $(x_i^2, 2x_iy_i, 2x_iz_i, y_i^2, 2y_iz_i, z_i^2)$. A least squares solution for the column vector \mathbf{T}_c can be obtained as follow: $\mathbf{T}_c=(\mathbf{M}^T \cdot \mathbf{M})^{-1} \cdot \mathbf{M}^T \cdot \mathbf{C}$.

Constrained Tractography: The Euler tractography algorithm⁴ was implemented using MATLAB 2010 and the diffusion tensor used for FOD calculation was adapted with the spatio-temporal correlation tensor through the Log-Euclidean metrics⁷: $\mathbf{D}_i'=\mathbf{D}_i+w\mathbf{T}_i$, where \mathbf{D}_i is original diffusion tensor, \mathbf{D}_i' is the adapted tensor used for Euler tracking, and w determines the weight of the spatio-temporal correlation tensor.

Seed points were randomly selected from left Wernicke's area which was defined using the method reported earlier⁸ and fiber tracking terminated when it reached the target of left Broca's area.

RESULTS

Tracking results using diffusion MRI, functional MRI and the proposed constrained method. It can be seen that the proposed method generated more rigid tracking fibers which clusters to construct more explicit neuronal fiber pathways. On the other hand, tracking results used diffusion MRI and functional MRI individually both generated irregular fibers. Meanwhile, both tracking seeds and terminates of the proposed method are also more aggregate together with high correlation between BOLD signal and stimuli.

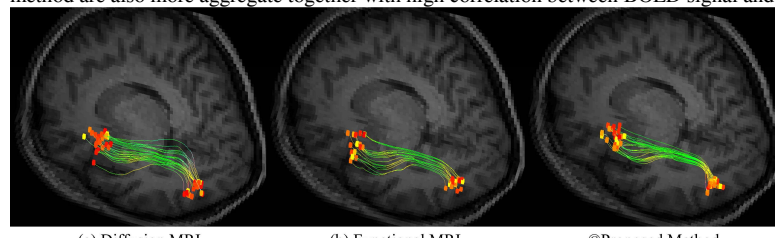


Figure 1. Tracking results using Euler method in diffusion MRI, spatio-temporal correlation tensor from functional MRI and the proposed method. Note that color of ROI dot demonstrates correlation between BOLD signal and stimuli, light yellow dot demonstrates high correlation and dark red dot corresponds to low correlation.

CONCLUSIONS

This work proposed an improved fiber tracking algorithm using spatio-temporal correlation tensor which characterizes local functional information to constrain the estimation of the local diffusion. This will produce more accurate tracking direction estimation thus benefit more rigid tracking results. Besides this, the proposed method introduced extra functional information to guide the diffusion MRI fiber tractography, which offers the potential of being used to map structure-functional relation more effectively.

ACKNOWLEDGEMENTS

NIH grant NS058639 (AWA)

REFERENCES

1. Ogawa S, et al. PNAS USA, 1990; 87:9868.
2. Ding Z, et al. PlosOne, 2013; in press.
3. Jones DK, et al. NMR Biomed, 2010; 23:803.
4. Basser PJ, et al. MRM, 2000; 44:41.
5. Arsigny V, et al. MRM, 2006, 56(2):411.
6. Morgan VL, et al. PlosOne, 2009, 4(8):e6660.